J Incl Phenom Macrocycl Chem (2011) 70:259–268
DOI 10.1007/s10847-010-9859-4

ORIGINAL ARTICLE

Host–guest association studied by fluorescence correlation spectroscopy

Mercedes Novo · Daniel Granadero · Jorge Bordello · Wajih Al-Soufi

Received: 26 June 2010 / Accepted: 5 September 2010 / Published online: 28 September 2010

Abstract Fluorescence Correlation Spectroscopy (FCS) is a powerful single molecule technique for the study of the stability and the association dynamics of supramolecular systems and, in particular, of host–guest inclusion complexes. With FCS the host–guest binding equilibrium constant is determined analysing the variation in the diffusion coefficient of the fluorescent guest or host with no need for a change in the photophysical properties of the fluorescent probe. FCS gives also access to the association/dissociation rate constants of the host–guest inclusion providing that the fluorescence intensity of host or guest changes upon complexation. These rate constants can be compared with that of a diffusion-controlled process estimated from the same FCS experiment allowing for a better understanding of the association dynamics. The results show that cyclodextrin cavities act as "hard" cages which put geometric and orientational restrictions on the inclusion of a hydrophobic guest, whereas micelles behave as "soft" cages without geometrical requirements.

In our contribution to this special issue we review briefly the application of FCS to the study of host–guest inclusion complexes with an emphasis on practical aspects and relevant bibliographic references.

Keywords Cyclodextrins · Micelles · Fluorescence correlation spectroscopy · Supramolecular association · Supramolecular dynamics

Introduction

Host–Guest complexes are supramolecular aggregates stabilized by non-covalent bonds and are ubiquitous in biochemical, pharmaceutical, environmental, cosmetic, food, and other chemical systems and applications [1]. Different approaches are necessary to fully understand a supramolecular system: structural studies yield stoichiometry, geometry, association sites and heterogeneity, thermodynamic studies provide information about stability, equilibrium constants and reversibility, and finally dynamic studies are necessary to describe the association/dissociation dynamics, diffusional properties or conformational dynamics. Most published studies focus on structure and thermodynamics of supramolecular association, which, however, give very few information about the dynamics of the system. As pointed out by Bohne "Dynamic studies are necessary to provide the 'movie' in addition to the 'snapshots' taken from structural and thermodynamic measurements" [2].

In this contribution we briefly summarize how to use Fluorescence Correlation Spectroscopy (FCS) for the study of supramolecular association and, more specifically, of the stability and the binding[1] dynamics in host–guest systems. We show how knowledge about the dynamics gives valuable information about the association mechanism, which is directly related to the structure of the host and the guest. For details we refer to relevant bibliography.

M. Novo (✉) · D. Granadero · J. Bordello · W. Al-Soufi
Department of Physical Chemistry, University of Santiago de Compostela, Biophysical Chemistry, Photophysics and Spectroscopy Group, 27002 Lugo, Spain
e-mail: m.novo@usc.es

[1] As usual we use "binding" as a general term for an attractive noncovalent interaction. In the context of "host–guest" systems it refers to a "complexation" or more specifically to "inclusion".

Association dynamics

Host–Guest complexes are typically formed by the association of host H with guest G to give a 1:1 complex HG (see Fig. 1). The association rate (on-rate) $v_+ = k_+$ [H] [G] is described by the bimolecular association rate constant k_+, whereas the dissociation rate (off-rate) $v_- = k_-$ [HG] is defined by the unimolecular dissociation rate constant k_-. Both processes, association and dissociation, are rate-limited by molecular diffusion and thus upper limits are given by diffusion-controlled rate constants: i.e. $k_+ < 10^{10}$ M^{-1} s^{-1}, $k_- < 10^9$ s^{-1} in aqueous solution.

At equilibrium both rates are equal, $v_+ = v_-$, and the binding equilibrium constant K is derived as ratio of the association and dissociation rate constants as given in Eq. (1).

$$K = \frac{[HG]_{eq}}{[H]_{eq}\,[G]_{eq}} = \frac{k_+}{k_-} \tag{1}$$

Dynamic studies give information on how fast the complex associates or dissociates. For a 1:1 complexation the corresponding rate law [Eq. (2)] and the typical condition of excess host concentration[2] ($[H]_0 \gg [G]_0$) lead to a pseudo-first order association rate and to kinetics which are mono-exponential with an observed relaxation rate constant k_R as given in Eq. (3).[3]

$$\frac{d[HG]}{dt} = k_+\,[H]\,[G] - k_-\,[HG] \tag{2}$$

$$[G](t) \sim e^{-k_R t}, \quad [HG]\,(t) \sim 1 - e^{-k_R t}, \quad k_R = k_+\,[H]_0 + k_- \tag{3}$$

The relaxation rate constant k_R depends on the two rate constants, k_+ and k_-. The contribution of the association process can be modulated by varying the host concentration $[H]_0$, but not that of the dissociation [3, 4].

Can we infer information about the relaxation rate constant k_R of the binding equilibrium from the corresponding equilibrium constant K? In other words: does knowledge about the stability (thermodynamics) of a complex give information about the dynamics of the host guest association? The answer is "not so much"; systems with similar values of their stability constant K may present very different values of their association and dissociation rate constants. For example, for a typical intermediate stability constant, $K = 1000$ M^{-1}, the association rate constant can fall in a very wide interval, between very low values, e.g. $k_+ = 10^3$ M^{-1} s^{-1} or very high ones, only limited by diffusion ($k_+ = 10^{10}$ M^{-1} s^{-1}), with the corresponding values of the dissociation rate constants as indicated in Fig. 2.

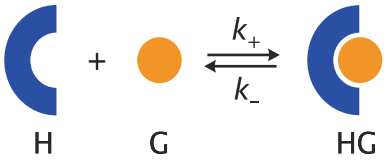

Fig. 1 Host H and guest G form complex HG with association rate constant k_+ and separate with dissociation rate constant k_-

That host–guest complexes with similar stability can present very different dynamics, had already been demonstrated by the classical work of Cramer et al. [5] for the inclusion of different azoderivatives by α-cyclodextrin (α-CD) studied by the temperature-jump technique. Substitution of the azoderivatives with ethyl or methyl side groups changes only very slightly the stability of the α-CD inclusion complex but decreases the association and dissociation rate constants by several orders of magnitude.

How fast is the association/dissociation process? The time scale of this process is given by the relaxation time $\tau_R = k_R^{-1}$ which is the inverse of the relaxation rate constant k_R [Eq. (3)]. Again, as an example, for $K = 1000$ M^{-1}, we can analyse the two above-mentioned cases as depicted in Fig. 3, right panel: slow dynamics with $k_+ = 10^3$ M^{-1} s^{-1}, $k_- = 1$ s^{-1} (upper red curve) correspond to long relaxation times of $\tau_R = 1$ s. Fast, diffusion-controlled dynamics with $k_+ = 10^{10}$ M^{-1} s^{-1}, $k_- = 10^7$ s^{-1} (lower, blue curve) lead to short relaxation times of $\tau_R = 100$ ns or faster. These

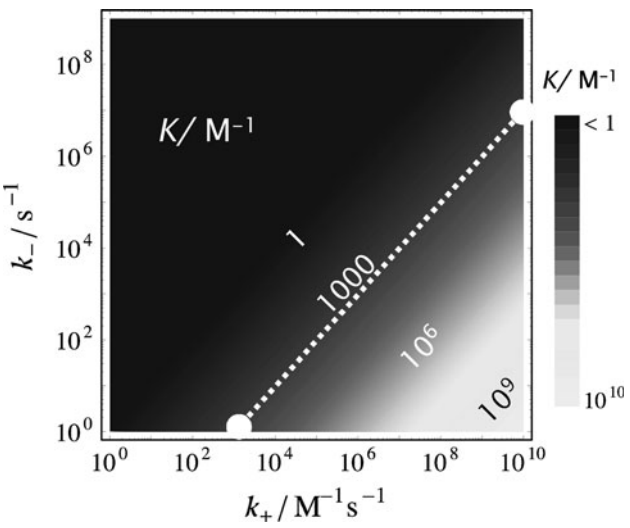

Fig. 2 Very different values of the association rate constant k_+ and the dissociation rate constant k_- can lead to the same value of the binding equilibrium constant K

[2] Here we assume that the guest acts as fluorescent probe. Being FCS a single molecule technique, the total concentration of the fluorescent probe is very low, of the order of $[G]_0 \approx 10^{-8}$ M. Thus, the condition ($[H]_0 \gg [G]_0$) is fulfilled even for hosts of low solubility or high affinity systems.

[3] Don't confuse the time dependence of the guest concentration [G](t) with the autocorrelation of the intensity fluctuations $G(\tau)$ defined in Eq. (4).

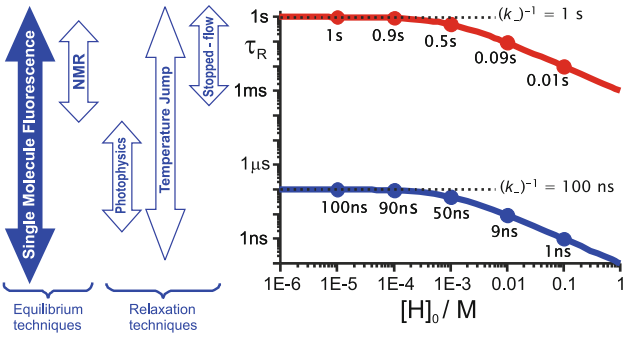

Fig. 3 *Right panel*: For the same typical intermediate binding equilibrium constant, $K = 1000\ M^{-1}$, the relaxation time $\tau_R = k_R^{-1}$ of the equilibrium can vary in a very wide time interval from seconds to nanoseconds. *Upper curve*: slow dynamics with $k_+ = 10^3\ M^{-1}\ s^{-1}$, $k_- = 1\ s^{-1}$, and $\tau_R < 1$ s. *Lower curve*: fast dynamics with $k_+ = 10^{10}\ M^{-1}\ s^{-1}$, $k_- = 10^7\ s^{-1}$, and $\tau_R < 100$ ns. *Left panel*: Dynamic range covered by some frequently used fast techniques for the determination of the rate constants of supramolecular association/dissociation

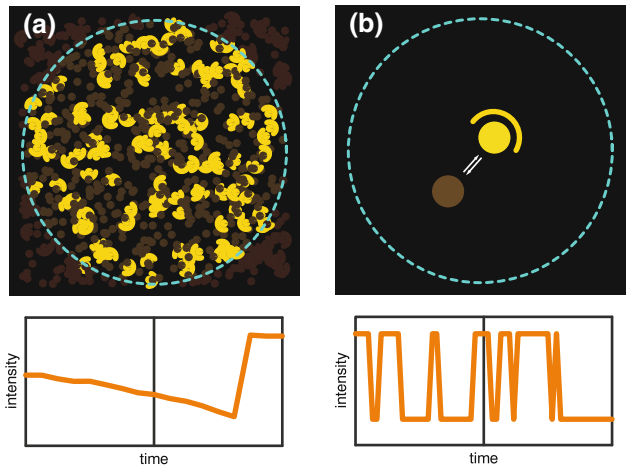

Fig. 4 Simulated kinetic experiments for the study the dynamics of a reversible (association) reaction assuming that the guest increases its fluorescence intensity upon complexation. *Upper panels*: scheme of the sample volume (*dashed circle*) with *bright* complex and *dark* free guest. *Lower panels*: observed total fluorescence intensity as function of time (time increases to the left). **a** Standard "bulk" measurement: the ensemble relaxes back to equilibrium after an external perturbation. The relaxation time is determined from the exponential change in the "bulk" fluorescence intensity. **b** Single molecule measurement: the system is at equilibrium and the reversible process is followed directly from the change in fluorescence intensity provoked by the reaction. Depending on the single molecule technique the rate constants k_+ and k_- are determined directly from the time the system stays in each of the two states (free, bound) or the relaxation time τ_R is determined from the characteristic time of the fluorescence fluctuations

relaxation rates correspond to conditions of very low host concentration where the dissociation process controls the relaxation rate. In both cases the observed relaxation time is shortened with increasing host concentration. As can be seen, binding dynamics cover a very wide time range and the upper limit corresponds to very fast reactions experimentally not easily accessible.

Frequently used fast techniques for the determination of the rate constants of supramolecular association/dissociation are temperature-jump (T-Jump), time-resolved fluorescence (TRF), laser flash photolysis (LFP), ultrasonic relaxation and stopped-flow (see Fig. 3, left panel) [2, 6–8]. These methods analyze the relaxation of the system back to equilibrium after a perturbation. TRF and LFP rely on the photophysics of chromophores with fluorescent excited states or long lived triplet states and/or on the presence of a quenching molecule. Ultrasonic relaxation needs no chromophore but requires detailed knowledge about the molecular process being disturbed. Laser T-Jump covers a wide time range from nanoseconds to seconds, whereas TRF, LFP and ultrasonic relaxation are limited to dynamics of nano- to microseconds. Stopped-flow techniques can only be used to study slow dynamics. There are other techniques that allow dynamic study of systems at thermodynamic equilibrium. The most known is NMR, which is, however, limited to slow dynamics.

Single molecule fluorescence

The study of supramolecular dynamics require methodologies which cover a very wide range of time scales, ideally within the same experiment. It is also preferred not to rely on unique photophysical properties of the host guest system and to avoid perturbation of the system. Techniques which analyze the fluorescence of single molecules have the potential to cover these needs. They analyze variations in the fluorescence intensity of a molecular system due to spontaneous fluctuations around the equilibrium, without the need for an external perturbation and they can cover a very wide dynamic range [9, 10].

Although standard "bulk" fluorescence experiments already use low dye concentrations of about 10^{-6} mol/L and small detection volumes around 1 mm^3, the observed fluorescence is still an average of the light emitted by about 10^{11} dye molecules! This huge number average hides any static and temporal heterogeneities in the molecular ensemble and, more important for our case, makes it practically impossible to follow directly the dynamics of the unsynchronized molecular processes. Kinetic measurements at these "bulk" concentrations require therefore some external perturbation which synchronizes the molecular processes, so that their relaxation back to equilibrium can be followed as a macroscopic variation of the ensemble properties (Fig. 4a).

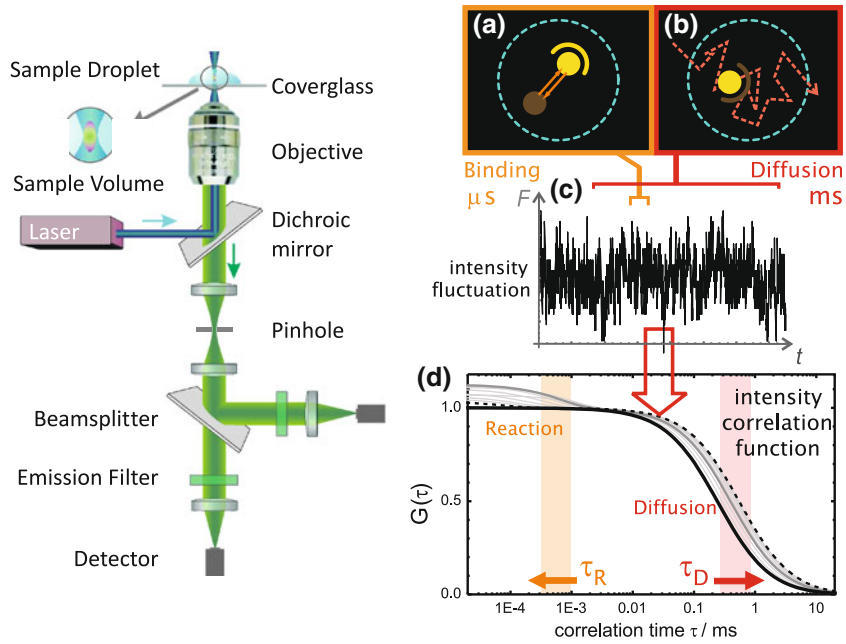

Fig. 5 Principles of Fluorescence Correlation Spectroscopy. *Left panel*: epi-illuminated confocal microscope used to create a microscopic sample volume. *Right panel*: scheme of the data analysis. **a**, **b** The *dashed circles* indicate the border of the sample volume. The *dots* represent dye molecules undergoing a reversible association (**a**), and moving randomly through the solution due to Brownian motion (**b**). Detected fluorescence intensity (**c**), and autocorrelation function of the intensity fluctuations (**d**)

Single molecule fluorescence techniques observe a very small number or even a single molecule at a time (Fig. 4b) and avoid thus the loss of information due to averaging. Observing a few molecules allows one to follow directly the dynamics of the reversible association process as significant fluctuations in the fluorescence intensity, provided that the association affects the brightness[4] of the fluorescent guest (or host).

In order to detect fluorescence from single fluorophores it is not sufficient to reduce the concentration of the observed dye but it is also necessary to suppress the background signal (Raman scattering, impurities) by reducing the sample volume itself. Different techniques are used for this aim. For slow dynamics one of the reaction partners is typically immobilized on a glass surface and the fluorescence is excited only within a very thin layer above this surface by means of special illumination techniques (e.g. total internal reflection, TIR). The fluorescence from this layer can then be detected with highly sensitive CCD cameras [9]. Dynamics in the microsecond to hour range can be observed, limited mainly by the photostability of the dyes at the long end and the time resolution of the detection at short times.

Faster dynamics are typically observed with molecules which diffuse freely through a very small open detection volume defined by the focus of an epi-illuminated confocal microscope (see Fig. 5). During the transit through the sample volume the fluorophore is repeatedly excited and the change in fluorescence intensity due to the reversible reaction is detected. Here the dynamic range is limited by the fluorescence lifetime of some nanoseconds of the dye itself and the mean transit time of the fluorophore through the sample volume, typically in the millisecond range. The fluorescence intensity fluctuations can be analyzed by different techniques, and we will present in the following FCS as one of the most widely used.

For all Single Molecule Fluorescence techniques several conditions have to be fulfilled. One needs very bright and photostable dyes, very efficient excitation and detection setups, very low dye concentrations and highly purified solvents and solutes. In order to observe the dynamics one also relies on a highly fluorescent probe molecule which undergoes some change in its photophysical properties during the association/dissociation process.

Fluorescence correlation spectroscopy

Principles

FCS analyzes the spontaneous temporal fluctuations of the fluorescence intensity emitted by a few (1–10) molecules in a small open sample volume. These intensity fluctuations may be due to various processes at the molecular level: changes in the singlet or triplet excited-state population, changes in the local concentration due to translational motion of the fluorophores in and out of the sample volume or changes in their physicochemical properties, for example due to a chemical reaction or, as in our case, supramolecular association. Each of these processes modulates

[4] The species dependent *brightness* is given by the product of the extinction coefficient, fluorescence quantum yield and detection efficiency and is a measure for the detected fluorescence count rate from each species.

the fluorescence intensity at a characteristic timescale which can in principle be derived from the autocorrelation function of the intensity trace. Several excellent reviews [11–15], monographs [9, 16–19], and textbooks [20, 21] present FCS theory for different applications. We will point out briefly the most important aspects.

In FCS the molecules under study diffuse freely freely within a small sample droplet and eventually pass through the focus of a confocal epi-illuminated fluorescence microscope (Fig. 5, left). The focus defines an open microscopic effective detection volume of some femtoliter (10^{-15} L). If the concentration of the dye molecules in the droplet is low (nanomolar, 10^{-9} mol/L) then only very few molecules are observed at a time. The molecules are excited by laser light through the microscope objective and their fluorescence is collected by the same objective and focused through a pinhole and filters onto detectors with single photon sensitivity. The molecules move randomly through the solution due to Brownian motion (Fig. 5b) and at the same time undergo a fast reversible reaction (Fig. 5a). Both processes introduce fluctuations at characteristic time scales in the detected total fluorescence intensity $F(t)$ (Fig. 5c). The characteristic time of the fluctuations is determined from the autocorrelation curve $G(\tau)$ of the intensity fluctuations $\delta F(t)$ (Fig. 5d) given by Eq. (4) with correlation time τ [3, 4].

$$G(\tau) = \frac{\langle \delta F\,(t) \cdot \delta F\,(t+\tau)\rangle}{\langle F\,(t)\rangle^2} \tag{4}$$

Under the conditions discussed in the following sections the full correlation function for translational diffusion and a fast reversible (association) reaction is given by Eq. (5) with the mean diffusion (transit) time $\bar{\tau}_D$, the mean number of fluorescent molecules in the sample volume N, the ratio between radial and axial radii of the sample volume w_{xy}/w_z, and the amplitude A_R of the reaction term.

$$G_{\mathrm{DR}}(\tau) = \frac{1}{N}\left(1+\frac{\tau}{\bar{\tau}_{\mathrm{D}}}\right)^{-1}\left(1+\left(\frac{w_{\mathrm{xy}}}{w_{\mathrm{z}}}\right)^2\frac{\tau}{\bar{\tau}_{\mathrm{D}}}\right)^{-\frac{1}{2}}\left(1+A_{\mathrm{R}}\,e^{-k_{\mathrm{R}}\tau}\right) \tag{5}$$

Translational diffusion

On the millisecond time scale the observed fluorescence intensity depends on the number of dye molecules present in the open sample volume, a number which fluctuates due to the entry and exit of dyes under Brownian motion. The characteristic time of these fluctuations reflects the mean transit (or diffusion) time τ_{D} of the fluorescent species through the sample volume, which depends on the translational diffusion coefficient of the fluorophore and on the size of the sample volume. A calibration of this size with a reference dye allows one then to determine the diffusion coefficient of the fluorophore from measurements of τ_{D}. The translational diffusion coefficient D is inversely proportional to the diffusion time τ_{D} according to Eq. (6), with w_{xy} being the radial radius of the sample volume. The diffusion coefficient D is also related to the hydrodynamic radius R_h as given for homogeneous spheres by the Stokes–Einstein relation on the right hand in Eq. (6), where k is the Boltzmann constant and η the viscosity of the solvent.

$$D = \frac{w_{xy}^2}{4\tau_D} = \frac{kT}{6\pi\eta R_h} \tag{6}$$

The amplitude of the correlation function [Eq. (5)] is inversely proportional to the number of fluorophores in the detection volume (N), which is a peculiarity of the technique: the lower the concentration of dye the higher the amplitude of the fluctuations and, consequently, of the correlation function.

Binding equilibrium constant

The diffusion coefficient of a fluorescent guest decreases when it binds to a host. The association of the guest to the host introduces a variation in the observed diffusion coefficient (or diffusion time) of the guest which depends on the third root of the molar mass ratio, as given by Eq. (7) for homogeneous compact spheres.

$$\frac{D_{HG}}{D_G} = \frac{\tau_G}{\tau_{HG}} \approx \frac{R_{h,G}}{R_{h,HG}} \approx \sqrt[3]{\frac{M_G}{M_{HG}}} \tag{7}$$

FCS is used here for binding dynamics that are much faster than the mean diffusion time of the fluorophore through the detection volume (fast exchange). In this case the fluorescent guests will associate and dissociate many times during their transit, changing rapidly between free (G) and bound (HG) state. The observed mean diffusion time $\bar{\tau}_D$ depends then on the fraction of the time that the fluorescent guests spent in the free or in the bound state. This can be expressed by the number-weighted mean diffusion coefficient $\bar{D}$ obtained from the individual coefficients D_G and D_{HG} of free and bound dye and the number fractions $X_x = N_x/(N_G + N_{HG})$as given in Eq. (8).

$$\bar{\tau}_D = \frac{w_{xy}^2}{4\bar{D}} \quad \bar{D} = X_G D_G + X_{HG} D_{HG} \tag{8}$$

In the case of the equilibrium of Fig. 1 and Eq. (1) the fractions can be expressed by the equilibrium constant K and the host concentration $[\mathrm{H}]_0$ which leads to Eq. (9).

$$\bar{\tau}_D([\mathrm{H}]) = \frac{\tau_G(1+K[\mathrm{H}]_0)}{1+\frac{\tau_G}{\tau_{HG}}K[\mathrm{H}]_0} \tag{9}$$

Titrations of this mean diffusion time at different host concentrations $[\mathrm{H}]_0$ allows one to determine the binding

equilibrium constant K and the limiting diffusion coefficients of free and bound guest [4].

The binding equilibrium constant K can be determined solely from the change in the hydrodynamic properties of the guest upon complexation. For the determination of K it is therefore not necessary (but allowed) that the fluorophore changes its brightness during the binding. This makes it possible to study nonfluorescent hosts labelled with a fluorophore which does not need to interact itself with the host. This is an advantage of FCS over other fluorescence techniques which rely on a significant change of some fluorescence properties of the guest in order to detect its binding.

An example is the inclusion of the nonfluorescent guest adamantane by β-CD [22]. The fluorescent label (Alexa 488) attached to the adamantane presents no change in its fluorescent properties due to the inclusion of the adamantane moiety by β-CD. The inclusion equilibrium is therefore not easily accessible by standard fluorescence techniques. A FCS titration, however, shows immediately a systematic increase of the diffusion time of the fluorescently labelled adamantane ($M_G = 826$ g mol^{-1}) on the addition of β-CD ($M_H = 1135$ g mol^{-1}), as shown in Fig. 6.

The experimentally determined ratio of the limiting values $D_{HG}/D_G = \tau_G/\tau_{HG} = 0.74$ coincides perfectly with the expected value $(M_G/M_{HG})^{1/3} = (0.422)^{1/3} = 0.75$ [see Eq. (7)] [22]. The equilibrium constant obtained from these FCS titrations is in good agreement with that obtained by other techniques.

In order to follow with FCS the relatively small variations in the diffusion coefficient D_{HG}/D_G observed with small hosts such as cyclodextrins great care has to be taken

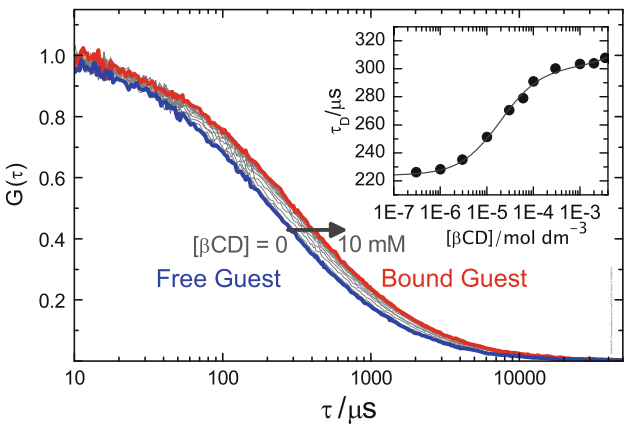

Fig. 6 Inclusion equilibrium between β-CD and adamantane labeled with Alexa 488 dye studied by FCS. Main panel: the diffusion term of the correlation curves shifts to longer times on the addition of increasing amounts of β-CD due to the increase in the mean diffusion time $\bar{\tau}_D$ of the guest. *Inset*: Plot of $\bar{\tau}_D$versus $[\beta\text{-CD}]_0$ (note the logarithmic concentration scale). Fitting of $\bar{\tau}_D$ with Eq. (9) yields the high equilibrium constant $K = (52 \pm 2)\ 10^3$ M^{-1} [22]

during the experiments and artefacts introduced by triplet-state population, saturation and photobleaching, background signal, variation in solvent viscosity, sample temperature and deformations of the effective detection volume (due, for example, to very small variations in the cover slide thickness) have to be taken into account [22–24].

For an accurate determination of the binding equilibrium constant it is very important to make sure that the observed diffusion time is not affected by saturation and photobleaching of the fluorophore due to too high excitation irradiance. The diffusion time has to be independent of the excitation power, both at zero and at high host concentrations, which has to be checked experimentally for each host–guest combination. Too high irradiance shortens the observed diffusion time as a function of the host concentration and leads to strongly erroneous results for the equilibrium constant.

Binding dynamics

Binding dynamics can be observed when the fluorescence brightness of the guest changes between its free and bound states. Binding leads then to fluorescence blinking which can be analysed by FCS. To be detectable in FCS the blinking must be much faster than the transit through the sample volume, that is the relaxation time τ_R of the binding process (Eq. (2)) must be shorter than the diffusion time τ_D (fast exchange). The fluorescence intensity fluctuations due to the binding dynamics introduce then an additional term in the correlation function (Eq. (5)) at the relaxation time τ_R with an amplitude A_R which depends strongly on the brightness ratio $q = Q_{HG}/Q_G$ of bound and free fluorophore (Fig. 7, insets τ_R and A_R). Again both τ_R and A_R can be expressed as function of the host concentration and the binding constant as given in Eqs. (10) and (11). [3]

$$\tau_R\ ([\mathrm{H}]) = (k_-\ (1 + K[\mathrm{H}]_0))^{-1} \tag{10}$$

$$A_R = \frac{K[\mathrm{H}]_0(1-q)^2}{(1+qK[\mathrm{H}]_0)^2} \tag{11}$$

The amplitude of the reaction term A_R is zero both at very low and at very high host concentrations when the guest is either totally free or fully bound (see Fig. 7). The highest amplitude A_R is reached at a host concentration $[\mathrm{H}]_{0,\max} = (K{\cdot}q)^{-1}$ which depends on the brightness ratio q. Fluorophores which increase strongly their brightness upon binding make it possible to detect the dynamics already at a very small degree of binding (low host concentrations) and at relatively long relaxation times [25].

From fits of the corresponding correlation function [Eqs. (5), (9), (10), (11)] to the experimental correlation curves one determines both the equilibrium constant K and the

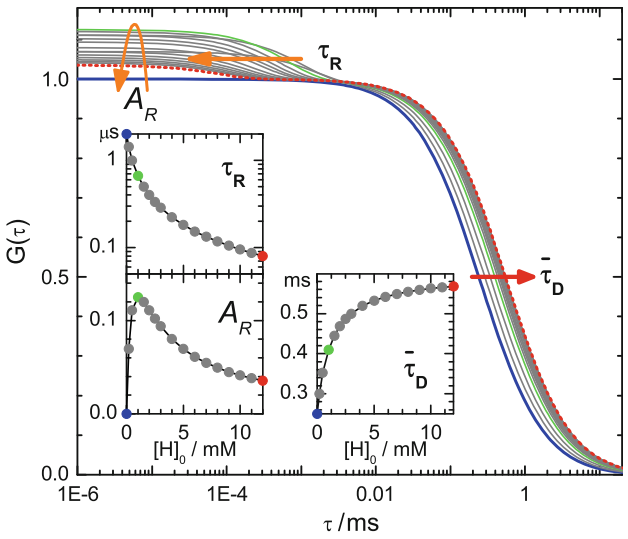

Fig. 7 *Main panel*: Correlation curves from simulated FCS experiments [Eq. (5)] of an inclusion equilibrium as depicted in Fig. 5. *Thick line*: free guest, $[H]_0 = 0$. *Thin grey lines*: intermediate host concentrations. *Dashed line*: highest host concentration $[H]_0 = 12$ mM. *Insets*: Dependence of the amplitude of the relaxation term A_R, of the relaxation time τ_R, and of the mean diffusion time $\bar{\tau}_D$ on $[H]_0$. (Parameters used for simulation: $N = 1$, $\tau_G = 0.25$ ms, $\tau_{HG} = 0.6$ ms, $q = 0.5$, $K = 2000$ M^{-1}, $k_+ = 10^9$ M^{-1} s^{-1}, $k_- = 5\ 10^5$ s^{-1})

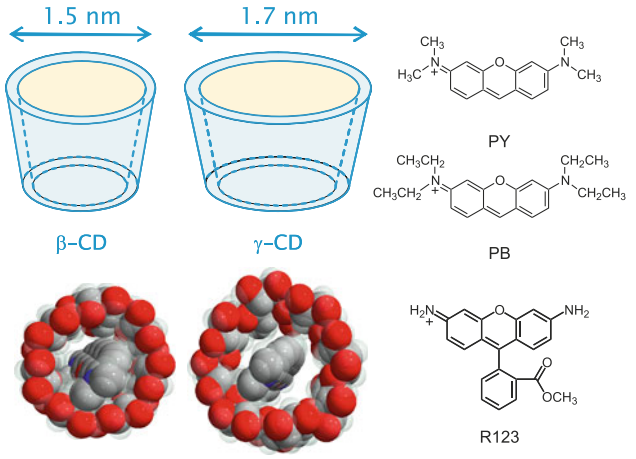

Fig. 8 Geometry of β-CD and γ-CD. Structures of the dyes PY, PB, and R123

dissociation rate constant k_-. From Eq. (1) also the association rate constant k_+ is obtained. [3]

Complications may arise when additional terms appear in the correlation curves, mainly due to excited-state dynamics of the fluorophore. Transitions in and out of the dark triplet state of the fluorophore introduce fluorescence fluctuations with the triplet lifetime of some microseconds [26]. The population of the triplet state is strongly dependent on the excitation power and can in principle be reduced working at low irradiance.

Influence of host–guest geometry on the dynamics

In order to study the influence of the geometry of host and guest on the binding dynamics we studied two parent cyclodextrins, β-CD and γ-CD, and two analogous guest molecules, pyronine Y (PY) and pyronine B (PB), which have the same xanthene skeleton but methyl and ethyl substituents, respectively, at the amino side groups (Fig. 8).

Electronic absorption and fluorescence spectroscopic studies showed that in all cases 1:1 pyronine:CD complexes are formed, although also 2:1 complexes with γ-CD are observed for both pyronines at dye concentrations much higher than those used in FCS [27, 28]. The values of the (1:1) association equilibrium constants, K, differ significantly between the four host–guest combinations (Table 1). In contrast to what may be expected, for each type of CD the binding constant is larger with PB than with PY in spite of the bulkier side groups of PB. Moreover, larger association equilibrium constants are obtained for the CD of smaller cavity.

The pure emission spectra of free and bound dyes allow one to estimate the brightness ratio q as given in Table 1. In the systems studied here, the brightness of the dyes decrease significantly when they are bound to the hosts.

As an example Fig. 9 shows a series of correlation curves obtained in titration experiments of PY with β-CD. Due to the fast exchange of the pyronine guest in and out of the CD complex only a single diffusion term with a mean diffusion time, $\bar{\tau}_D$, is observed which increases as the host concentration is increased (compare insets $\bar{\tau}_D$ in Figs. 7, 9). The second term in the correlation curves due to the association/dissociation dynamics is described by the relaxation time, τ_R, and an amplitude A_R that varies with the concentration of the host as expected (compare insets τ_R in Figs. 7, 9). In all cases it has to be checked that the relaxation time is in fact much shorter than the diffusion time, in order to allow for the separation of the two terms in the correlation function. The small contribution of the triplet-state formation to the correlation curves which appears at about the same correlation time as the reaction term must also be taken into account in the analysis.

Global target analysis of the FCS curves as a function of host concentration with the correlation function as given in Eq. (5) yields the association/dissociation rate constants [3]. The results of the fits for the systems under study are shown in Table 1. In most cases the value of K obtained from bulk fluorescence and absorption titrations was fixed in the fits of the correlation curves, in order to improve the accuracy of other fit parameters such as k_-. For the system PY:γ-CD it was not possible to determine the association and dissociation rate constants since the reaction term

Table 1 Results from Global target fits of series of FCS curves and derived values as explained in the text [3, 4]

	PB:β-CD	PY:β-CD	PB:γ-CD	PY:γ-CD	R123:TX100
$K/10^3$ M^{-1}	2.1 ± 0.2	0.40 ± 0.04	0.19 ± 0.03	0.04 ± 0.01	65 ± 3
q	0.49 ± 0.04	0.6 ± 0.2	0.67 ± 0.02	0.34 ± 0.02	0.42 ± 0.03
τ_A/ms	0.30 ± 0.02	0.25 ± 0.02	0.27 ± 0.02	0.23 ± 0.02	0.263 ± 0.002
τ_B/ms	0.40 ± 0.04	0.45 ± 0.06	0.46 ± 0.05	0.41 ± 0.05	1.66 ± 0.05
$k_+/10^9 M^{-1} s^{-1}$	**0.15 ± 0.05**	**0.2 ± 0.1**	**0.56 ± 0.11**	**>1**	**14 ± 1**
$k_-/10^4 s^{-1}$	7.6 ± 2.7	50 ± 30	300 ± 30	–	22 ± 1
$k_d/10^9 M^{-1} s^{-1}$	**7.7 ± 0.5**	**8.0 ± 0.5**	**8.0 ± 0.5**	**8.4 ± 0.3**	**16 ± 1**
$k_{-d}/10^9$ s^{-1}	2.0 ± 0.1	2.6 ± 0.2	2.1 ± 0.2	2.7 ± 0.1	0.11 ± 0.01
$k_r/10^9$ s^{-1}	0.04 ± 0.01	0.07 ± 0.03	0.16 ± 0.03	–	–
$k_{-r}/10^4$ s^{-1}	7.7 ± 2.7	50 ± 30	320 ± 100	–	–
$D_G/10^{-10} m^2$ s^{-1}	4.8 ± 0.4	5.8 ± 0.4	4.8 ± 0.4	5.8 ± 0.4	4.3 ± 0.4
$D_{HG}/10^{-10}$ m^2 s^{-1}	3.6 ± 0.4	3.2 ± 0.3	3.1 ± 0.4	3.5 ± 0.4	0.7 ± 0.1
R_G/R_{HG} (Å)	5.1/6.8	4.2/7.6	5.1/7.8	4.2/7.0	5.7/36
$M_{w,G}/M_{w,HG}$ (Da)	324/1459	267/1402	324/1621	267/1564	381/95000

The diffusion coefficients D and all derived values were recalculated for a new reference value for Rhodamine 6G, $D_{R6G}(25\ °C) = (4.0 \pm 0.3)\ 10^{-10}\ m^2\ s^{-1}$ [29, 30]. The uncertainties represent one standard deviation as given by the fits and do not include the uncertainty in the reference value. All values given for 25 °C. The molar mass does not include that of the counterions of the charged dyes

As a guide for the eye the association rate constant and the diffusion controlled rate constant are set in bold

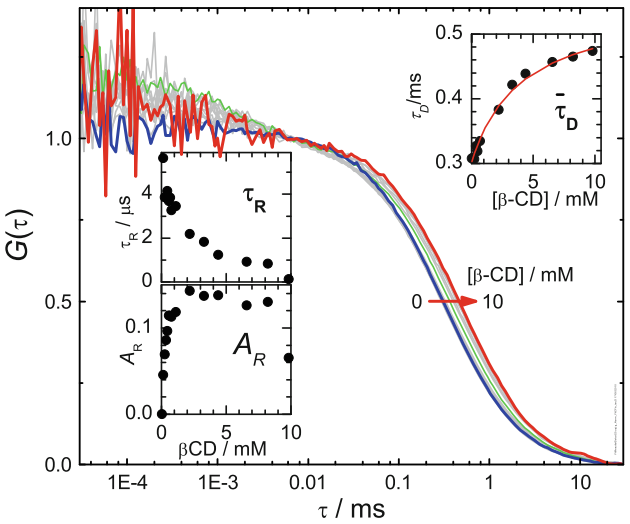

Fig. 9 *Main panel*: Experimental normalized correlation curves of PY in aqueous solution with increasing β-CD concentrations. *Insets*: Variation of the mean diffusion time τ_D, the relaxation time τ_R and the amplitude of the reaction term A_R with the concentration of β-CD as determined from individual fits of Eq. (5) [3]

appears at too short correlation times overlapping with the fluorescence lifetime of PY.

From the hydrodynamic properties of host and guest the collision rate constants k_d for a purely diffusion-controlled association process between two species can be estimated applying the Smoluchowski equation [Eq. (12)] as given in Table 1.

$$k_d = 4\pi\ (D_G + D_H)\ (R_G + R_H)\ N_0 \qquad (12)$$

(D_G, R_G and D_H, R_H are diffusion coefficients and hydrodynamic radii of guest G and host H, respectively, and N_0 is the Avogadro constant.) This diffusion limited rate constant k_d will be compared later with the rate constant k_+ of association between guest and host determined from the same FCS data. It is clearly an advantage of FCS to yield in the same measurement information about both diffusional and association dynamics.

Binding dynamics of "hard" and "soft" cages

The rate constants k_+ of association of the guests PY and PB to β-CD are both similar with a very high value of about $k_+ = 0.2 \times 10^9\ M^{-1}\ s^{-1}$ (Table 1). This is, however, still about 40 times lower than the estimated collision rate constant $k_d = 8 \times 10^9\ M^{-1}\ s^{-1}$, with which host and guest collide due to Brownian motion in the solvent (Eq. (12), Table 1). The overall association (inclusion) is thus much slower than expected for a diffusion-controlled process. This can be understood on the basis of a two step process (see Fig. 10a) [3]. First host and guest collide with rate constant k_d and form an encounter complex within a common solvent cage. If no specific interactions are assumed a lifetime of the encounter complex of about 1 ns can be estimated. During this lifetime host and guest collide of the order of 100 times changing randomly their relative orientation. In most cases they separate again with rate constant k_{-d} without inclusion. Depending on the geometrical requirements for the inclusion of the guest into the host a small fraction of the relative orientations may be

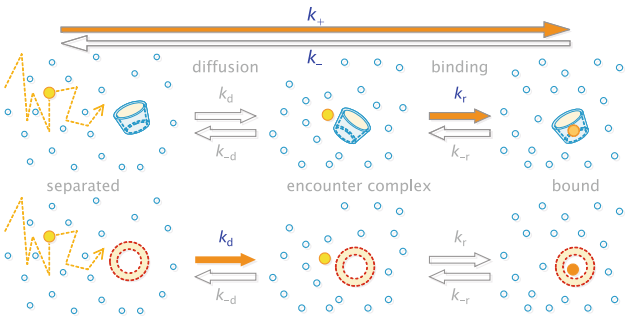

Fig. 10 Two step mechanism for supramolecular association involving the formation of an encounter complex, for a "hard" cage (cyclodextrin) (**a**) and a "soft" cage (micelles) (**b**)

favourable so that inclusion can occur with a rate constant of inclusion, k_r. The overall association rate is thus mostly controlled by this inclusion step.

Both guests, PY and PB, have similar association rate constants in spite of their different side groups. On one hand, simulations indicate that the side groups may not change significantly the critical dimension which determines the probability to enter the β-CD cavity [3] and, on the other hand, the high flexibility of the CD molecule probably allows for an induced fit compensating part of the difference in the guest geometry [31].

Another interesting result is the fact that the difference in the stability of these inclusion complexes is determined by their dissociation and not by the association process. The dissociation rate constants of PY and PB with β-CD (Table 1) differ in about one order of magnitude, reflecting the stronger interaction of PB than PY with the interior of the β-CD cavity, as already proposed on the basis of "bulk" fluorescence studies [32].

What happens if we increase the size of the host cavity? The data for the inclusion of PY and PB by γ-CD, a host with a 20 % bigger diameter of its cavity, show that the association rate constant, k_+, of the PB:γ-CD complex is about four times higher than in the case of PB:β-CD (Table 1). The wider γ-CD cavity increases the fraction of favourable relative orientations which lead to an inclusion, although the association process is still not diffusion controlled.

However, the wider cavity weakens also the specific interactions between host and included guest resulting in a strongly increased dissociation rate constant. The overall stability of the pyronine/γ-CD complexes is therefore much lower than that of the pyronine/β-CD complexes.

What do we expect for hosts without geometric restrictions? Micelles are themselves highly dynamic supramolecular self-assemblies of surfactants. Dyes such as the xanthene dye, rhodamine 123 (R123) exchange dynamically between the aqueous and the micellar pseudophase in a process similar to the inclusion described before. But, as opposed to the cyclodextrins, the micelle presents no geometric restrictions for the association of the dye; they act as "soft" hosts.

R123 is a typical probe for FCS, and is very suitable for dynamic studies in micellar systems since it presents a partition equilibrium between the aqueous phase and the micellar pseudophase formed by neutral micelles such as those formed by the aggregation of a well-known non-ionic surfactant, Triton X-100 (TX100) (Fig. 8). [4, 33, 34]. The 1:1 binding equilibrium constant for the partition equilibrium of the R123 with TX100 micelles is given in Table 1. Due to the low dye concentrations an occupancy number of more than one dye molecule per micelle is negligible.

A strong change in the brightness of R123 during the association process to TX100 micelles makes it possible to follow the association dynamics with FCS as described before (Table 1) [4, 25, 33]. As expected, the rate constant of the association of R123 to a TX100 micelle is as fast as the diffusion-controlled collision rate constant itself: $k_+ \approx k_d \approx 15 \times 10^9\ \mathrm{M}^{-1}\ \mathrm{s}^{-1}$. This shows that the association is diffusion controlled, in accordance with the picture of an unspecific association without orientational or geometrical requirements (see Fig. 10b). In this sense, the micelles may be seen as "soft" cages, as opposed to the cyclodextrin "hard" cages, which, although highly flexible, impose orientational restrictions to the inclusion.

Acknowledgments MN and WAS thank the Xunta de Galicia and the Ministerio de Educación y Ciencia for financial support (CTQ2007-68057-C02-02/BQU, INCITE09E2R209064ES, INCITE09262304PR, 2009/029). J. B. thanks the Ministerio de Educación y Ciencia for a research scholarship.

References

1. Dodziuk, H.: Introduction to Supramolecular Chemistry. Springer, Dordrecht (2002)
2. Bohne, C.: Supramolecular dynamics studied using photophysics. Langmuir. **22**, 9100–9111 (2006)
3. Al-Soufi, W., Reija, B., Novo, M., Felekyan, S., Kühnemuth, R., Seidel, C.A.M.: Fluorescence correlation spectroscopy, a tool to investigate supramolecular dynamics: inclusion complexes of pyronines with cyclodextrin. J. Am. Chem. Soc. **127**, 8775–8784 (2005)
4. Al-Soufi, W., Reija, B., Felekyan, S., Seidel, C.A., Novo, M.: Dynamics of supramolecular association monitored by fluorescence correlation spectroscopy. Chemphyschem. **9**, 1819–1827 (2008)
5. Cramer, F., Saenger, W., Spatz, H.C.: Inclusion compounds. XIX. The formation of inclusion compounds of alpha-cyclodextrin in aqueous solutions. Thermodynamics and kinetics. J. Am. Chem. Soc. **89**(1), 14–20 (1967). doi:10.1021/ja00977a003
6. Kleinman, M.H., Bohne, C.: Use of photophysical probes to study dynamic processes in supramolecular structures. In: Ramamurthy, V., Schanze, K.S. (eds.) Organic Photochemistry, p. 391. Marcel Dekker Inc, New York (1997)
7. Pace, T.C.S., Bohne, C.: Dynamics of guest binding to supramolecular systems: techniques and selected examples. Adv. Phys. Org. Chem. **42**, 167–223 (2008)

8. Zana, R.: Dynamics of Surfactant Self-Assemblies: Micelles, Microemulsions, Vesicles, and Lyotropic Phases. Taylor & Francis/CRC Press, Boca Raton (2005)
9. Selvin, P.R., Ha, T.: Single-Molecule Techniques: A Laboratory Manual. Cold Spring Harbor Laboratory Press, Cold Spring Harbor (2008)
10. Walter, N.G., Huang, C.Y., Manzo, A.J., Sobhy, M.A.: Do-it-yourself guide: how to use the modern single-molecule toolkit. Nat. Methods. **5**, 475–489 (2008)
11. Widengren, J., Rigler, R.: Fluorescence correlation spectroscopy as a tool to investigate chemical reactions in solutions and on cell surfaces. Cell. Mol. Biol. **44**, 857–879 (1998)
12. Van Craenenbroeck, E., Engelborghs, Y.: Fluorescence correlation spectroscopy: molecular recognition at the single molecule level. J. Mol. Recognit. **13**, 93–100 (2000)
13. Krichevsky, O., Bonnet, G.: Fluorescence correlation spectroscopy: the technique and its applications. Rep. Prog. Phys. **65**, 251–297 (2002)
14. Hess, S.T., Huang, S., Heikal, A.A., Webb, W.W.: Biological and chemical applications of fluorescence correlation spectroscopy: a review. Biochemistry. (N. Y.) **41**, 697–705 (2002)
15. Gösch, M., Rigler, R.: Fluorescence correlation spectroscopy of molecular motions and kinetics: advances in fluorescence imaging: opportunities for pharmaceutical science. Adv. Drug Deliv. Rev. **57**, 169–190 (2005)
16. Thompson, N.L.: Fluorescence correlation spectroscopy. In: Lakowicz, J.R. (ed.) Topics in Fluorescence Spectroscopy. Techniques, p. 337. Plenum Press, New York (1991)
17. Rigler, R., Elson, E.S.: Fluorescence Correlation Spectroscopy: Theory and Applications. Springer Verlag, Berlin (2001)
18. Zander, C., Enderlein, J., Keller, R.A.: Single-Molecule Detection in Solution—Methods and Applications. VCH-Wiley, Berlin (2002)
19. Gell, C., Brockwell, D., Smith, A.: Handbook of Single Molecule Fluorescence Spectroscopy. Oxford University Press, Oxford (2006)
20. Valeur, B.: Molecular Fluorescence: Principles and Applications. Wiley-VCH, Weinheim (2002)
21. Lakowicz, J.R.: Principles of Fluorescence Spectroscopy. Springer, New York (2006)
22. Granadero, D., Bordello, J., Pérez-Alvite, M.J., Novo, M., Al-Soufi, W.: Host-guest complexation studied by fluorescence correlation spectroscopy: adamantane–cyclodextrin inclusion. Int. J. Mol. Sci. **11**, 173–188 (2010)
23. Enderlein, J., Gregor, I., Patra, D., Fitter, J.: Art and artefacts of fluorescence correlation spectroscopy. Curr. Pharm. Biotechnol. **5**, 155–161 (2004)
24. Enderlein, J., Gregor, I., Patra, D., Dertinger, T., Kaupp, U.B.: Performance of fluorescence correlation spectroscopy for measuring diffusion and concentration. Chemphyschem. **6**, 2324–2336 (2005)
25. Bordello, J., Novo, M., Al-Soufi, W.: Exchange-dynamics of a neutral hydrophobic dye in micellar solutions studied by fluorescence correlation spectroscopy. J. Colloid Interface Sci. **345**, 369–376 (2010)
26. Widengren, J., Mets, U., Rigler, R.: Fluorescence correlation spectroscopy of triplet states in solution: a theoretical and experimental study. J. Phys. Chem. **99**, 13368–13379 (1995)
27. Reija, B., Al-Soufi, W., Novo, M., Vázquez Tato, J.: Specific interactions in the inclusion complexes of pyronines Y and B with beta-cyclodextrin. J. Phys. Chem. B **109**, 1364–1370 (2005)
28. Bordello, J., Reija, B., Al-Soufi, W., Novo, M.: Host-assisted guest self-assembly: enhancement of the dimerization of pyronines Y and B by gamma-cyclodextrin. Chemphyschem. **10**, 931–939 (2009)
29. Gendron, P.O., Avaltroni, F., Wilkinson, K.J.: Diffusion coefficients of several rhodamine derivatives as determined by pulsed field gradient-nuclear magnetic resonance and fluorescence correlation spectroscopy. J. Fluoresc. **18**, 1093–1101 (2008)
30. Müller, C.B., Eckert, T., Loman, A., Enderlein, J., Richtering, W.: Dual-focus fluorescence correlation spectroscopy: a robust tool for studying molecular crowding. Soft Matter. **5**, 1358–1366 (2009)
31. Dodziuk, H.: Rigidity versus flexibility. A review of experimental and theoretical studies pertaining to the cyclodextrin nonrigidity. J. Mol. Struct. **614**, 33–45 (2002)
32. Almgren, M., Wang, K., Asakawa, T.: Fluorescence quenching studies of micellization and solubilization in fluorocarbon-hydrocarbon surfactant mixtures. Langmuir. **13**, 4535–4544 (1997)
33. Novo, M., Felekyan, S., Seidel, C.A.M., Al-Soufi, W.: Dye-exchange dynamics in micellar solutions studied by fluorescence correlation spectroscopy. J. Phys. Chem. B **111**, 3614–3624 (2007)
34. Freire, S., Bordello, J., Granadero, D., Al Soufi, W., Novo, M.: Role of electrostatic and hydrophobic forces in the interaction of ionic dyes with charged micelles. Photochem. Photobiol. Sci. **9**, 687–696 (2010)